

2024

Investigation of Hot-Spots Due to Trapped Flux in Niobium Superconducting Radiofrequency Cavities

B. Khanal

Old Dominion University, bkhanal@odu.edu

P. Dhakal

Thomas Jefferson National Accelerator Facility

Follow this and additional works at: https://digitalcommons.odu.edu/physics_fac_pubs



Part of the [Engineering Physics Commons](#)

Original Publication Citation

Khanal, B., & Dhakal, P. (2024). Investigation of hot-spots due to trapped flux in niobium superconducting radiofrequency cavities. In F. Pilat, W. Fischer, R. Saethre, P. Anisimov, & I. Andrian (Eds.), *Proceedings of the 15th International Particle Accelerator Conference* (pp. 2768-2771). JACoW Publishing.
<https://doi.org/10.18429/JACoW-IPAC2024-WEPS34>

This Conference Paper is brought to you for free and open access by the Physics at ODU Digital Commons. It has been accepted for inclusion in Physics Faculty Publications by an authorized administrator of ODU Digital Commons. For more information, please contact digitalcommons@odu.edu.

INVESTIGATION OF HOT-SPOTS DUE TO TRAPPED FLUX IN NIOBIUM SUPERCONDUCTING RADIOFREQUENCY CAVITIES*

B.D. Khanal[†], Department of Physics, Old Dominion University, Norfolk, VA, USA
P. Dhakal, Thomas Jefferson National Accelerator Facility, Newport News, VA, USA

Abstract

One of the significant sources of residual losses in superconducting radio-frequency cavities is magnetic flux trapped during the cool-down due to the incomplete Meissner effect. If the trapped vortices are non-uniformly distributed on the cavity surface, the temperature mapping revealed the “hot-spots” at the location of high density of pinned vortices. Here, we performed a rf test on 1.3 GHz single cell cavity with the combination of the temperature mapping system. The temperature mapping revealed the development of the hot spots with the increase in rf field inside the cavity. When magnetic field is trapped locally on the surface of cavity, the hot-spots strength increase rapidly, showing the direct correlation of vortex induced hot spot and corresponding rf loss.

INTRODUCTION

Superconducting radio-frequency (SRF) niobium cavities are the fundamental device to accelerate the charged particles (electrons, positrons, proton, antiprotons, and heavy ions) close to the velocity of light transferring radio-frequency (rf) energy to the beams. The performance of the SRF niobium cavities are measured in terms of quality factors $Q_0 = \frac{G}{R_s}$ as a function of accelerating gradient E_{acc} , where G depends on geometry of the cavity and R_s is the average inner surface resistance. Since SRF cavities can attain high-quality factor in the range of $Q_0 > 10^{10} - 10^{11}$, the vast majority of large particle accelerators in operation or under construction are using SRF cavities [1]. Recent advances in the processing of bulk niobium cavities have resulted in significant improvement of the quality factor and reducing R_s via diffusion of impurities over a few micrometers on the inner surface of the cavities [2–5]. However, one of the most outstanding issues are the trapped vortices during the transition of the cavity from normal to superconducting state. The trapped vortices oscillate by rf field, thereby dissipating rf power [6]. This dissipation increases temperature of the inner surface of the cavity. The thermal maps of the SRF cavity during the rf test detect the regions of high rf loss, referred as “hot-spots”. The main sources of these hot-spots may be nonuniform impurities or oxide distributions, surface roughness, grain boundaries [7]. Additionally, temperature mapping (T-map) manifest the overheated regions in the high magnetic field area of cavities [7]. In this study, we have characterized the

regions of high magnetic field density to demonstrate the vortex induced hot spots.

EXPERIMENTAL SETUP

A single cell TESLA shaped [8] 1.3 GHz cavity fabricated from high purity Nb was used for this study. After fabrication, the cavity was subjected to $\sim 150 \mu\text{m}$ electropolishing, followed by $800^\circ\text{C}/3\text{h}$ heat treatment. The cavity was again subjected to $\sim 50 \mu\text{m}$ electropolishing. Standard practice of cavity processing steps such as, high pressure rinse with de-ionized water, drying in ISO 4 clean room and clean room assembly were done before the rf tests.

The cavity was assembled with T-map system as shown in Fig. 1, which consist of 36 boards each consists of 16 sensors rely on 100Ω Allen-Bradely carbon resistors at each 10° azimuth angle of elliptical cavity. The details of temperature mapping system can be found in Ref. [9, 10]. Additionally, a solenoid coil with 10 turns and ($\sim 10 \text{ mm}$) made from 38 AWG enameled copper wire was attached at the cavity surface encircling 3rd and 4th temperature sensors of temperature board at 10° . The coil produce the magnetic field locally at the surface of the cavity. Two cernox sensors were mounted at the top iris, and two Cernox sensors were mounted at the bottom iris of the cavity each 180° apart to monitor the temperature. One flux gate magnetometer (FGM) was attached on the centre of the coil perpendicularly and one FGM was attached at upper beamtube of the cavity to measure the residual magnetic field at the Dewar.

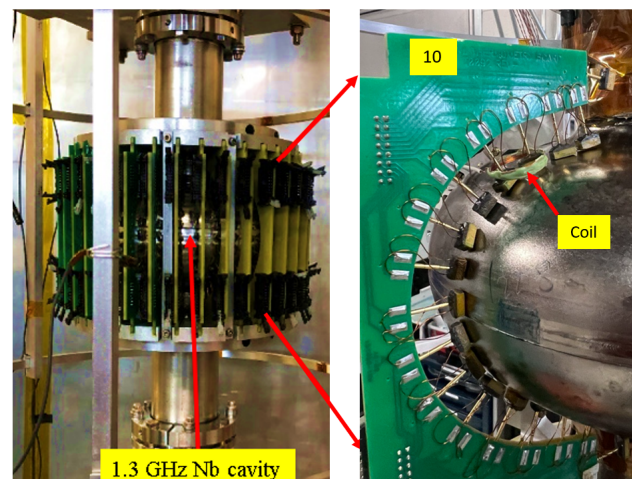


Figure 1: The temperature map setup around the cavity.

After the installation of coil and T-map, (i) the cavity was put on the Dewar and maintain the magnetic field $\leq 3 \text{ mG}$ with the help of compensation coils inside the Dewar. During

* The work is partially supported by the U.S. DOE, Office of science, Office of High Energy Physics under Awards No. DE-SC 0009960. This manuscript has been authored by Jefferson Science Associates, LLC under U.S. DOE Contract No. DE-AC05-06OR23177.

[†] bkhan001@odu.edu

the cool down through the transition temperature (T_c), the temperature difference between top iris to bottom iris was maintained ≤ 0.1 K. (ii) The calibration of carbon resistors was done during $R_s(T)$ measurement at $B_p \sim 15$ mT from 4.34 K to 1.6 K. (iii) Once the calibration was done $Q_0(E_{acc})$ at 2.0 K and T-maps were measured. (iv) The cavity was warmed-up above T_c and repeated the step (ii)-(iv) with ~ 20 mG and ~ 40 mG. The next test consisted of warm up of the Dewar above T_c and maintain the residual field in the Dewar ≤ 2 mG. A current of 200 mA was applied to the coil that was mounted on the cavity surface, producing ~ 100 μ T magnetic field perpendicular to the cavity surface as measured by FGM. Again, the cavity was cooled down with less than 0.1 K temperature difference between the cavity irises in order to maximize the flux trapping. When the cavity reached superconducting state (~ 4.2 K), the current to the coil is switched off. The magnetic field reading after the current being turned off is the amount of magnetic field trapped on the cavity surface. It was found that about 40 % of the magnetic flux is trapped on the cavity surface. The steps (ii)-(iv) were repeated.

EXPERIMENTAL RESULTS

RF Results

Figure 2 shows the $R_s(1/T)$ from 4.3 - 1.6 K at $B_p \sim 15$ mT. The data were fitted with the method described in Ref. [11] to extract the temperature independent resistance, R_i . The linear fits of R_i vs. applied field results in the flux trapping sensitivity of 0.22 n Ω /mG consistent with previous results [12].

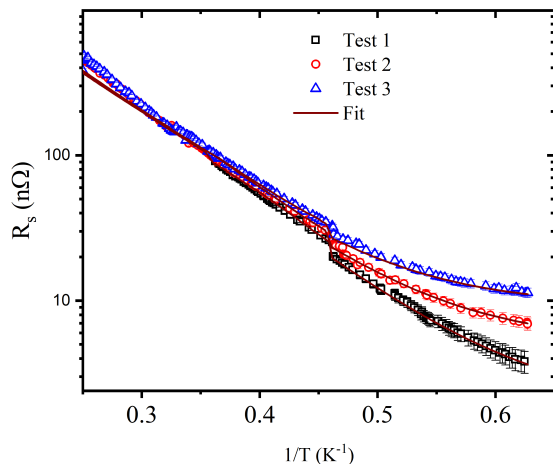


Figure 2: $R_s(T)$ at $B_p \sim 15$ mT with residual field 3, 20 and 40 mG trapped. The solid line is the fit using method described in Ref. [11].

Figure 3 shows the $Q_0(E_{acc})$ measured for 4 different flux trapping condition. The test labeled test 1 is after the first cooldown with < 3 mG residual flux during the cooldown. Test 4 represents the rf test after the locally trapped magnetic field. All rf tests were limited by high field Q-slope.

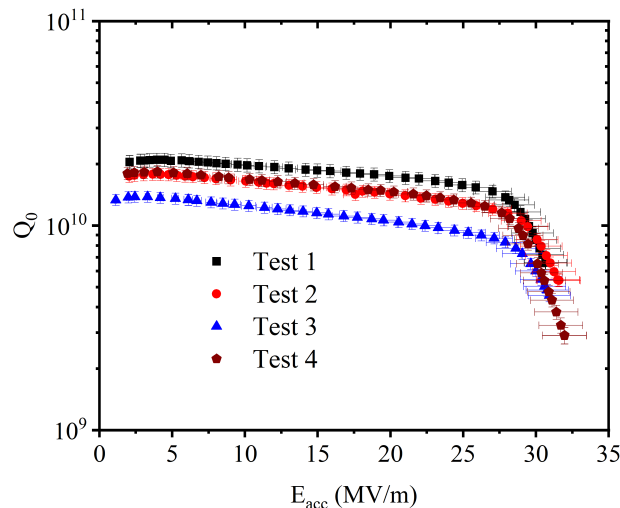


Figure 3: $Q_0(B_p)$ measured at 2 K for different condition of trapped magnetic field. All rf tests were limited by high field Q-slope.

Temperature Mapping

Figure 4 shows the temperature map at highest accelerating gradient for uniform flux trapping. Few hot-spots were appeared in the temperature maps and the strength of hot-spots increase with the increase in trapped flux. For examples, the Sensor # 6 at angular positions 120° and 130°, clearly indicate the strongest hot-spots.

Figure 5 shows the ΔT of selected hot-spot of sensor # 6 at 120° as a function of rf peak magnetic field. The ΔT showed $\sim B_p^2$ dependence until $B_p \approx 120$ mT which follow ohmic-type heating and rapidly increases for $B_p > 120$ mT with higher ΔT with increase in trapped magnetic field. The field at which the average temperature increase rapidly corresponds to the onset of high field Q-slope as shown in Fig.3.

The test # 4 consists of setting the residual magnetic field in Dewar ≤ 2 mG and apply a local magnetic field on the cavity surface using a coil encircling sensors # 3 and 4 at azimuth angle 10°. Figure 6 shows the temperature map at $E_{acc} \approx 31$ MV/m. Also shown is the ΔT of the previously found hot spots along with the newly created hotspots. Clearly, the temperature reading by sensor # 4 on angle 10° represents the strongest hot-spot. This shows the clear evidence of vortex induced hot-spots. The ΔT shows the strong B_p dependence compared to the hotspots during global flux trapping. Additional rf test was repeated by moving the coil at different locations and confirmed the migration of vortex induced hot-spots similar to previous report on 3 GHz cavity [13].

DISCUSSION AND SUMMARY

We have measured the flux trapping sensitivity on 1.3 GHz single cell cavity by applying the magnetic field during the cooldown. The flux trapping sensitivity was found to

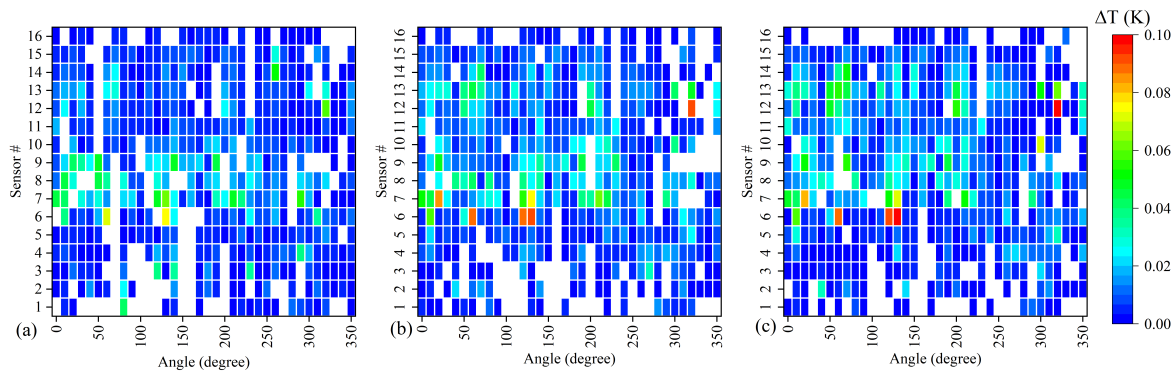


Figure 4: Temperature map at $E_{acc} \approx 31$ MV/m for (a) 3 mG, (b) 20 mG and (c) 40 mG residual flux trapping. The whiteout area represents faulty sensors.

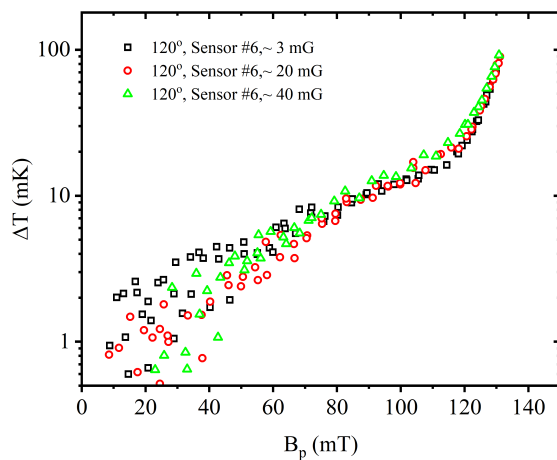


Figure 5: $\Delta T(B_p)$ as a function of peak rf magnetic field at for a hotspot during rf test.

be $0.22 \text{ n}\Omega/\text{mG}$ when the field is trapped globally. The rf test when magnetic field is trapped at localized locations of cavity suggest that the overall $Q_0(E_{acc})$ has the similar dependence when the magnetic flux is trapped on the whole cavity surface, even though the density of the vortices may be different depending on the location. Furthermore, this study confirms that high field Q-slope is not significantly impacted by the magnitude and location of trapped magnetic flux [13–15].

The temperature mapping during the global flux trapping reveals the location of the hot-spots distributed along the cavity surface. The strength of the hot-spots increases with the increasing trapped magnetic field suggest that the density of vortices at hot-spots increases with the increase in trapped magnetic field. Further studies are planned to use the magnetic field scanning system to quantify the amount of flux trapped at the hot-spots [16].

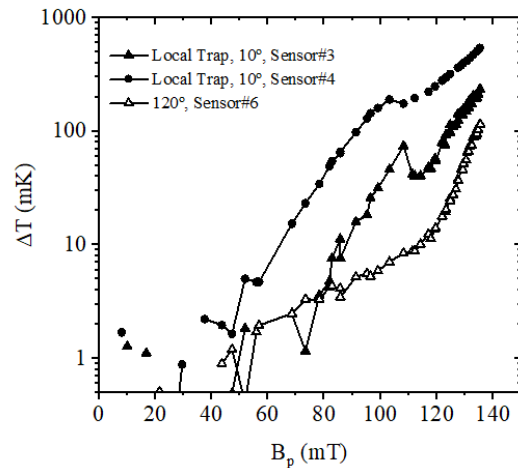
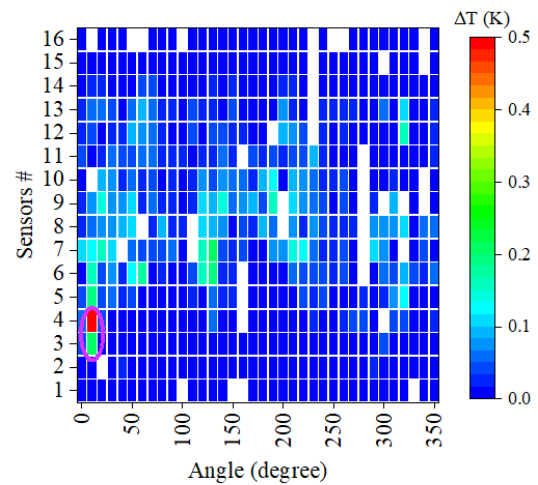


Figure 6: Temperature map at $E_{acc} \approx 31$ MV/m (top) and ΔT of selected hot-spot as a function of B_p during test #4. The oval on the T-map represents the coil mounted on the cavity surface producing the local magnetic field.

ACKNOWLEDGEMENTS

We would like to acknowledge Peter Owen for RF and Justin Kent for cryogenic support as well as technical staff members for the cavity fabrication, processing and assembly.

REFERENCES

- [1] H. Padamsee, J. Knobloch and T. Hays. “*RF superconductivity for accelerators*”, New York, NY, USA: John Wiley & Sons, Feb. 2008.
- [2] P. Dhakal *et al.*, “Effect of high temperature heat treatments on the quality factor of a large-grain superconducting radio-frequency niobium cavity”, *Phys. Rev. ST Accel. Beams*, vol. 16, pp. 042001, Apr. 2013.
doi:10.1103/PhysRevSTAB.16.042001
- [3] A. Grassellino *et al.*, “Nitrogen and argon doping of niobium for superconducting radio frequency cavities: a pathway to highly efficient accelerating structures”, *Supercond. Sci. Technol.*, vol. 26, pp. 102001, Aug. 2013.
doi:10.1088/0953-2048/26/10/102001
- [4] A. Grassellino *et al.*, “Unprecedented quality factors at accelerating gradients up to 45 MV/m in niobium superconducting resonators via low temperature nitrogen infusion” *Supercond. Sci. Technol.*, vol.30, pp. 094004, Aug. 2017.
doi:10.1088/1361-6668/aa7afe
- [5] P. Dhakal, “Nitrogen doping and infusion in SRF cavities: A review”, *Physics Open*, vol. 5, pp. 100034, Aug. 2020.
doi:10.1016/j.physo.2020.100034
- [6] A. Gurevich and G. Ciovati, “Effect of vortex hotspots on the radio-frequency surface resistance of superconductors” *Phys. Rev. B*, vol. 87, pp. 054502, Feb. 2013.
doi:10.1103/PhysRevB.87.054502
- [7] G. Ciovati and A. Gurevich, “Evidence of high-field radio-frequency hot spots due to trapped vortices in niobium cavities”, *Physical Review Special Topics-Accelerators and Beams*, vol. 11, pp. 122001, Dec. 2008.
doi:10.1103/PhysRevSTAB.11.122001
- [8] B. Aune *et al.*, “Superconducting TESLA cavities”, *Physical Review special topics accelerators and beams*, vol. 3, pp. 092001, Sep. 2000.
doi:10.1103/PhysRevSTAB.3.092001
- [9] J. Knobloch, H. Muller, and H. Padamsee, “Design of a high speed, high resolution thermometry system for 1.5 GHz superconducting radio frequency cavities”, *Rev. Sci. Instrum.*, vol. 65, pp. 3521–3527, Nov. 1994.
doi:10.1063/1.1144532
- [10] G. Ciovati *et al.*, “Temperature mapping system for single cell cavities”, Jefferson Lab, Newport News, VA, USA, Rep. JLAB-TN-05-059, 2005.
- [11] G. Ciovati, P. Dhakal, and A. Gurevich, “Decrease of the surface resistance in superconducting niobium resonator cavities by the microwave field”, *Appl. Phys. Lett.*, vol. 104, pp. 092601, Mar. 2014. doi:10.1063/1.4867339
- [12] P. Dhakal, G. Ciovati and A. Gurevich “Flux expulsion in niobium superconducting radio-frequency cavities of different purity and essential contributions to the flux sensitivity”, *Phys. Rev. Accel. Beams*, vol. 23, pp. 023102, Feb. 2020.
doi:10.1103/PhysRevAccelBeams.23.023102
- [13] B.D. Khanal, G. Ciovati, and P. Dhakal, “Quench Detection in a Superconducting Radio Frequency Cavity with Combined Temperature and Magnetic Field Mapping”, in *Proc. SRF’23*, Grand Rapids, MI, USA, Jun. 2023, pp. 211-215.
doi:10.18429/JACoW-SRF2023-MOPMB045
- [14] K. Howard, D. Bafia, A. Grassellino, and Y.K. Kim, “Exploration of Parameters that Affect High Field Q-Slope”, in *Proc. SRF’23*, Grand Rapids, MI, USA, Jun. 2023, pp. 178-182.
doi:10.18429/JACoW-SRF2023-MOPMB037
- [15] I. Parajuli, G. Ciovati, and A. Gurevich, “Magneto-thermal limitations in superconducting cavities at high radio-frequency fields”. *Front. Electron. Mater.*, vol. 4, pp. 1339293, Mar. 2024.
doi:10.3389/femat.2024.1339293
- [16] I. P. Parajuli, G. Ciovati and J. Delayen, “High resolution diagnostic tools for superconducting radio frequency cavities”, *Rev. Sci. Instrum.*, vol. 93, pp. 113305, Nov. 2022.
doi:10.1063/5.0117868